PASJ: Publ. Astron. Soc. Japan **54**, 61–71, 2002 February 25

Observations of SiO Maser Sources within a Few Parsec from the Galactic Center

Shuji DEGUCHI
Nobeyama Radio Observatory, National Astronomical Observatory, Minamimaki, Minamisaku, Nagano 384-1305
deguchi@nro.nao.ac.jp
Takahiro FUJII
Institute of Astronomy, The University of Tokyo, Mitaka, Tokyo 181-0015
fujii@mtk.ioa.s.u-tokyo.ac.jp
Makoto MIYOSHI
VERA Office, National Astronomical Observatory, Mitaka, Tokyo 181-8588
miyoshi@miz.nao.ac.jp
and
Jun-ichi NAKASHIMA
Department of Astronomical Science, The Graduate University for Advanced Studies,
Nobeyama Radio Observatory, Minamimaki, Minamisaku, Nagano 384-1305
junichi@nro.nao.ac.jp

(Received 2001 May 17; accepted 2001 October 24)

Abstract

Mapping and monitoring observations of SiO maser sources near the Galactic center were made with the Nobeyama 45-m telescope at 43 GHz. Rectangular mapping an area of approximately $200'' \times 100''$ in a $30''$ grid, and triangular mapping in a $20''$ grid toward the Galactic center, resulted in 15 detections of SiO sources; the positions of the sources were obtained with errors of 5–$10''$, except for a few weak sources. Three-year monitoring observations found that the component at $V_{\rm lsr} = -27\,{\rm km\,s^{-1}}$ of IRS 10 EE flared to about 1.5 Jy during 2000 March–May, which was a factor of more than 5 brighter than its normal intensity. Using the radial velocities and positions of the SiO sources, we identified 5 which are counterparts of previously observed OH 1612 MHz sources. The other 10 SiO sources have no OH counterparts, but two were previously detected with VLA, and four are located close to the positions of large-amplitude variables observed at near-infrared wavelengths. A least-squares fit to a plot of velocities versus Galactic longitudes gives a rather high speed for the rotation of the star cluster around the Galactic center. The observed radial-velocity dispersion is roughly consistent with a value obtained before. It was found that all of the SiO sources with OH 1612 MHz counterparts have periods of light variation longer than 450 days, while SiO sources without OH masers often have periods shorter than 450 days. This fact suggests that lower-mass AGB stars are more often detected in SiO masers than in the OH 1612 MHz line.

Key words: Galaxy: center — Galaxy: nucleus — masers — stars: late-type

1. Introduction

The Galactic-center star cluster consists of mixed stellar populations (Krabbe et al. 1995; Morris, Serabyn 1996). It involves a number of late-type stars which are potential candidates for OH/SiO maser emitters. Deep surveys in OH 1612 MHz, H_2O 22 GHz, and SiO 43 GHz masers (Sjouwerman et al. 1998b; Menten et al. 1997; Izumiura et al. 1998) have been made; a dozen sources have been detected within a few parsec of the Galactic center. The accurate H_2O/SiO maser positions of these sources observed by the Very Large Array (VLA) provided a precise alignment between the near-infrared and radio coordinate frames (Menten et al. 1997), enabling the position of Sgr A* to be pinpointed with an accuracy better than $0.''1$ on near-infrared images. Detections of accelerating motions of stars near the Galactic center fixed the mass of the cental object at about $3 \times 10^6\,M_\odot$ (Ghez et al. 2000). Because radio interferometers have a potential of measuring the proper motions of stars relative to Sgr A* [e.g., Sjouwerman et al. (1998a)] more accurately than the present optical/infrared telescopes (Genzel et al. 1996; Eckart, Genzel 1997), to detect more SiO maser sources near the Galactic center and to investigate their properties will be quite important.

Using the 45-m telescope at Nobeyama, Izumiura et al. (1998) detected 14 SiO sources around the Galactic center. These observations (by a beam width of about $40''$) proved that the SiO maser source density is peaked at the Galactic center. Because this was a set of pointed observations toward the Galactic center and two one-beam offset positions, the SiO source positions were not determined with an accuracy better than the beam size. To remedy the positional uncertainties to some degree, we made new mapping observations of SiO masers near the Galactic center using the 45-m telescope in the year 2000. The present mapping observations on a $30''$ grid can be used to derive the source positions with an uncertainty of about 5–$10''$, depending on the signal-to-noise ratio. Also, because the intensities of SiO masers are expected to vary strongly on a time scale of one year, we monitored the intensities of SiO masers toward the Galactic center during 1999–2001. During the three-year monitoring observations,

we found an SiO maser flare in the $-27\,\mathrm{km\,s^{-1}}$ component of IRS 10 EE in 2000 March–June. We present the details of these observations in this paper.

2. Observations

Simultaneous observations of the SiO $J = 1$–0, $v = 1$ and 2 transitions at 43.122 and 42.821 GHz, respectively, were made with the 45-m radio telescope at Nobeyama on 1999 June 8–12, 2000 May 20–29, and 2001 February 9. A cooled SIS receiver (S40) with a bandwidth of about 0.4 GHz was used, and the system temperature (including atmospheric noise) was 200–250 K (SSB). The aperture efficiency of the telescope was 0.60 at 43 GHz. The half-power beam width (HPBW) was about $38''$ at 43 GHz. A factor of $2.9\,\mathrm{Jy\,K^{-1}}$ was used to convert the antenna temperature to flux density. An acousto-optical spectrometer array of low resolution (AOS-W) was used. Each spectrometer had 250 MHz bandwidth and 2048 channels, giving a velocity coverage of about $1700\,\mathrm{km\,s^{-1}}$ and a spectral resolution of $1.7\,\mathrm{km\,s^{-1}}$ (per two binned channels). Observations were made in a position-switching mode, and the off-position was chosen to be $10'$ away from the Galactic center in azimuth. The telescope pointing was checked using a strong SiO maser source, OH 2.6–0.4. The calibration of the telescope antenna temperature was made by observing the intensities of the ^{29}SiO (thermal), H52α (recombination), U42.767, and SiO $J = 1$–0, $v = 1$ (maser) lines toward Sgr B2 MD5 [e.g., Shiki et al. (1997)]. The total on-source integration time was approximately 2 hours per day.

In the 1999 June observations, only the direction toward Sgr A* was observed; (R.A., Decl., epoch) = ($17^{\mathrm{h}}42^{\mathrm{m}}29\overset{\mathrm{s}}{.}314$, $-28^\circ59'18\overset{''}{.}3$, 1950) (Rogers et al. 1994). At this time, we spent three days looking for extreme velocity components ($|V_{\mathrm{lsr}}| > 350\,\mathrm{km\,s^{-1}}$); no extreme velocity component above 0.04 and 0.03 K for the $J = 1$–0, $v = 1$ and 2 transitions, respectively, was detected in the frequency range between 42.73–43.35 GHz (approximate velocity span ranging from -2200 to $2700\,\mathrm{km\,s^{-1}}$ for the SiO $J = 1$–0 $v = 1$ transition). In fact, several unidentified lines were found in the spectra toward Sgr B2 MD5 in this frequency range: U42.767, U43.018, U43.026, and U43.178. These U-lines should appear at $V_{\mathrm{lsr}} = 378\,\mathrm{km\,s^{-1}}$ for the $J = 1$–0 $v = 2$ transition, and $V_{\mathrm{lsr}} = 723$, 668, and $-390\,\mathrm{km\,s^{-1}}$ for the $J = 1$–0 $v = 1$ transition, if the circumnuclear molecular ring (cf., Wright et al. 2001) contains a sufficient number of molecules responsible for these U-lines. The spectra toward the Galactic center above $|V_{\mathrm{lsr}}| > 350\,\mathrm{km\,s^{-1}}$ were carefully checked for contamination by these lines, but we found no such feature at the corresponding velocities (except for weak features due to ^{29}SiO, H52α, and U42.767 at several $10'$ offset positions from Sgr A*).

In the 2000 May observations, we made mapping observations in an area covering approximately $200'' \times 100''$ centered toward Sgr A*. Two different modes of mapping were used: 3-point (triangular) mapping with $20''$ separation toward Sgr A*, and 9-point (3×3 square) mappings toward $(\Delta l, \Delta b) = (0'' \text{ or } \pm 60'', 0'')$ on a $30''$ grid. The 9-point mapping mode was utilized to obtain a reasonably high level of signals in one run of the typical mapping time of about two hours (approximately 10-minutes integration per point). The mapped points are shown in the top panel of figure 1. The large circle in figure 1 indicates the effective beam of the telescope (HPBW $\sim 40''$). Because the telescope pointing has been known to be influenced strongly by wind, we made 3-point mapping on those days with wind speed less than $5\,\mathrm{m\,s^{-1}}$, when the telescope pointing was excellent (error $\lesssim 5''$ accuracy), and 9-point mapping on relatively windy days with wind speeds of 5–10 $\mathrm{m\,s^{-1}}$ (approximately $\lesssim 10''$ accuracy). Because the grid separation is larger than HPBW in the 9-point mapping, the relative intensities of the SiO maser components in the grid points were supposed to be kept constant, even though the wind velocity was slightly high. In the 2001 February observations, we could manage only a few hours of observation time, and we made observations in the 3-point mapping mode toward Sgr A*; the signal-to-noise ratio of the spectra obtained was not very high. Therefore, we averaged the spectra of three positions (a half-beam width each away). They are shown at the bottom in figure 2.

A shallow survey of SiO sources in the Galactic center area was also made with the 45-m telescope using a multibeam receiver (S40M) prior to the present observations (2000 March–April). This shallow observation detected 9 sources in the $7' \times 13'$ area toward the Galactic center (Miyazaki et al. 2001). The present observations concentrated on a smaller and much closer area to the Galactic center with a longer integration time per point and using a more sensitive single-beam receiver, S40.

As noted in Izumiura et al. (1998), the AOS-W spectra toward the strong continuum source, Sgr A* (~ 11 Jy at 43 GHz; Sofue et al. 1986 ; Beckert et al. 1996), exhibited a baseline distortion of about 0.3 K at the maximum, and ripples due to a standing wave in the telescope system. The ripples in the velocity range of $\pm 350\,\mathrm{km\,s^{-1}}$ were relatively weak. In order to remove these complex ripple features from the spectra, we took running means of the spectra (average of about 100 channels, or about $80\,\mathrm{km\,s^{-1}}$ width), and the averaged spectra were subtracted from the originals. With this procedure, the baselines of the resulting spectra became quite flat. Because the SiO maser lines are quite narrow (width less than $10\,\mathrm{km\,s^{-1}}$) and weak ($T_{\mathrm{a}} < 0.2$ K), this method seems to work well, except for a strong line of $T_{\mathrm{a}} \sim 0.5$ K at $-27\,\mathrm{km\,s^{-1}}$ (No. 6 in table 1). An additional baseline adjustment was made by taking a parabolic fit to the trough between $\pm 40\,\mathrm{km\,s^{-1}}$ near this strong feature. The resulting three-year spectra toward Sgr A* [$(\Delta l, \Delta b) = (0, 0)$] are shown in figure 2.

Detections were judged by criteria similar to those given in Izumiura et al. (1998). All of the peaks for a single channel with S/N > 3 and features for several channels with $(\mathrm{S/N})_{\mathrm{broad}} > 5$ were treated as detection candidates. Then, all of the features were checked as to whether or not they were detected in the spectra of both the $v = 1$ and 2 transitions of SiO, at nearby positions, or at different epochs of observations. Dubious features were discarded. After these careful checks, we selected 15 SiO spectral components as confident detections, which are listed in table 1; the number, telescope positions (relative to Sgr A*), V_{lsr}, peak antenna temperatures, integrated intensities, r.m.s. noise values, and signal-to-noise ratios integrated over the emission profile, are given. We show the spectra of the detected sources in figures 3, 4,

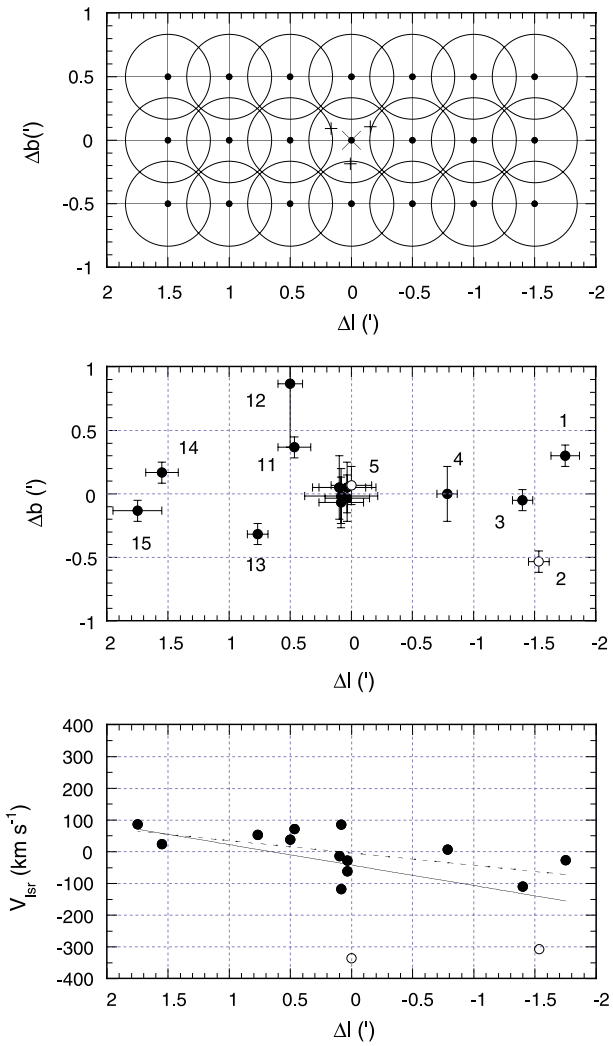

Fig. 1. Mapped positions of the telescope (top), positions of the 15 detected sources with error bars (middle), and position–velocity diagram of the detected sources (bottom). The coordinates, Δl and Δb, indicate position differences from Sgr A* in Galactic coordinates in unit of arcminute. The extreme sources with $|V_{\rm lsr}| > 300\,{\rm km\,s^{-1}}$ are shown as open circles in the middle and bottom panels. The numbers in the middle panel correspond to the SiO source number in tables 1 and 2. The solid and broken lines in the bottom panel are least-squares linear fits for all sources and for all but the extreme sources, respectively.

and 5. The components at -117 and $-337\,{\rm km\,s^{-1}}$ were quite weak and only slightly above the critical level of detections in 2000 May. These components were detected at several different positions and epochs. They were, in fact, more clearly detected previously: the $-117\,{\rm km\,s^{-1}}$ component in 1999, and the $-338\,{\rm km\,s^{-1}}$ component in 1997 (Izumiura et al. 1998). For the $-117\,{\rm km\,s^{-1}}$ component (No. 9) in figure 3, the spectra taken in 1999 are shown.

3. Discussion

3.1. Source Positions and Identifications

Because most of the components were detected at more than one telescope position, we computed the most likely positions of the SiO features from the relative intensities at the several observed positions. We assumed that the antenna temperature of a SiO maser component varies with the angular separation from the telescope pointing center according to the Gaussian beam shape with HPBW = 40″ (which is taken to be slightly larger than the nominal HPBW because of pointing fluctuation due to wind). The most likely position of a component was calculated by minimizing the sum, $\Sigma[(F_{\rm obs} - F_{\rm exp})/T_{\rm rms}]_i^2$, where the sum was made over the detected and undetected ($F_{\rm obs} = 0$) positions, i; $F_{\rm obs}$, $F_{\rm exp}$, and $T_{\rm rms}$ are the observed integrated intensity of the component, the expected integrated intensity of the component at the observed position assuming the Gaussian beam shape, and the r.m.s. noise temperature, respectively. The errors in Δl and Δb are also calculated from the distance which gives twice the minimum value of the above sum. The resulting most-likely positions obtained are given in table 2; the component number, Galactic longitude and latitude, the relative positions from Sgr A*, errors of positions, SiO radial velocity (averaged in $J = 1$–0, $v = 1$ and 2 transitions), the reference and name of the previously detected sources, the radial velocity in the literature, and the separation of the positions from the identified source are given. The obtained positions are plotted in the middle panel in figure 1 with uncertainty bars.

The identifications were made by using both the positions and radial velocities. A list of the previously detected OH 1612 MHz sources near the Galactic center (Sjouwerman et al. 1998b) was used for the identification. The positions for these OH sources are known to an accuracy of better than $\sim 1''$. Previous identifications of SiO sources with OH sources were also made by Izumiura et al. (1998). No. 6 in table 2 is the OH/IR source, 359.946−0.048 (IRS 10 EE; Menten et al. 1997), which has a radial velocity of $-27\,{\rm km\,s^{-1}}$. The location of this source is well known from near-infrared, OH, and SiO maser observations (Menten et al. 1997; Sjouwerman et al. 1998b). The position obtained in the present paper agrees well with the OH position within an accuracy of about 6″. The high signal-to-noise ratio of this component confirms that this method for determining the positions of SiO masers works nicely. Source No. 10 with $V_{\rm lsr} = -13\,{\rm km\,s^{-1}}$ has been identified as IRS 15 NE (Menten et al. 1997) with the VLA; the VLA position agrees with the position obtained in the present paper within an error of 5″. The positions of the other 4 weaker sources (No. 2, 11, 13, and 15) also coincide well with the positions of the identified OH sources within accuracies of 3–10″, thus verifying this method for weaker sources.

The radial velocity of SiO source No. 4, $V_{\rm lsr} = 7\,{\rm km\,s^{-1}}$, is close to the center velocity of the OH 1612 MHz double peaks of OH 359.931−0.050, (Sjouwerman et al. 1998b) at $V_{\rm lsr} = 17.5\,{\rm km\,s^{-1}}$ (the expansion velocity is about $14\,{\rm km\,s^{-1}}$). Because the SiO position obtained is separated from the OH position by 11″, it is probably a different source. The position of SiO source No. 8 ($85\,{\rm km\,s^{-1}}$) agrees well with that of OH 359.947−0.046, which is known to an accuracy of 4″ (but note that there is a large uncertainty in the SiO position). However, the radial velocity of the SiO masers, $85\,{\rm km\,s^{-1}}$, is slightly outside of the OH double-peak velocities (89.4 and $105.3\,{\rm km\,s^{-1}}$). Therefore, we left these two SiO sources unassigned.

It is not surprising that more than half of the SiO maser sources have no OH 1612 MHz counterpart. Previous studies of SiO masers near the Galactic center (Lindqvist et al. 1991)

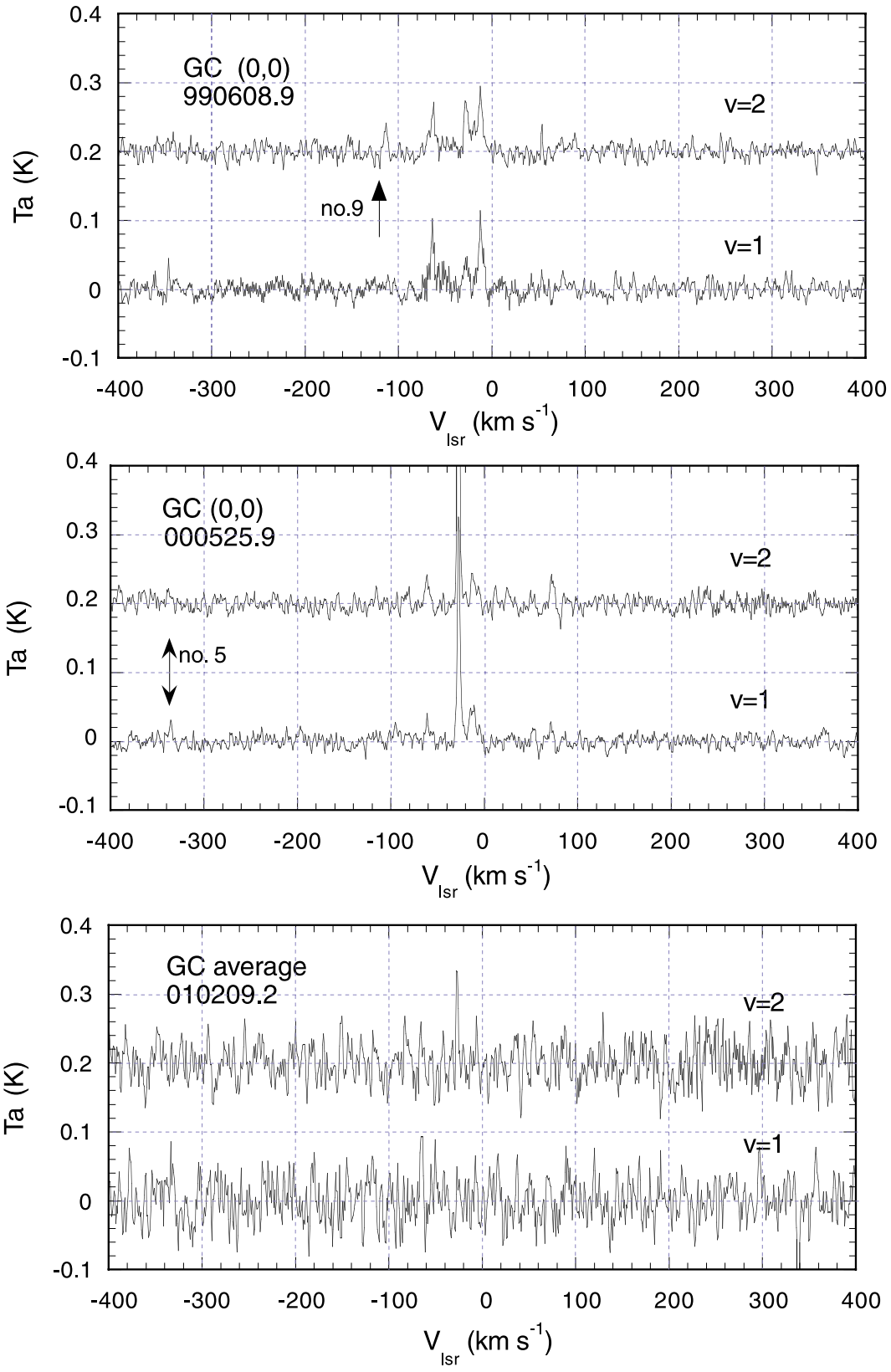

Fig. 2. Time variation of the SiO maser spectra toward Sgr A*. The data were taken on 1999 June 8 (top), 2000 May 25 (middle), and 2001 February 9 (bottom). In fact, the bottom spectra are averages over the three 12″-offset spectra taken in the 3-point mapping mode to improve S/N.

Table 1. Observed Line Parameters.

		$J = 1$–0, $v = 1$					$J = 1$–0, $v = 2$					
No.	$(\Delta l, \Delta b)^*_{\rm obs}$ ($''$, $''$)	$V_{\rm lsr}$ (km s^{-1})	$T_{\rm a}$ (K)	F (K km s^{-1})	$T_{\rm rms}$ (K)	S/N	$V_{\rm lsr}$ (km s^{-1})	$T_{\rm a}$ (K)	F (K km s^{-1})	$T_{\rm rms}$ (K)	S/N	Date (yymmdd)
1	(−90, 30)	−26.0	0.096	0.368	0.019	7.4	−27.4	0.084	0.496	0.021	7.2	000530
2	(−90, −30)	−308.0	0.668	2.764	0.018	55.1	−308.3	0.403	2.173	0.021	33.3	000530
3	(−90, 0)	−110.2	0.172	0.700	0.019	13.6	−110.1	0 .144	0.775	0.023	10.7	000530
4	(−60, 0)	6.3	0.109	0.436	0.018	8.8	7.4	0.087	0.296	0.014	8.5	000530
5	(0, 0)	−335.8	0.031	0.123	0.009	5.2	−335.7	0.044	0.314	0.014	6.1	000525
6	(0, −12)	−27.8	0.349	1.228	0.008	59.8	−27.4	0.583	1.732	0.010	72.3	000526
7	(0, 0)	−60.8	0.102	0.206	0.012	9.0	−62.0	0.109	0.243	0.014	8.6	000525
8	(0, −12)	85.2	0.073	0.265	0.008	12.4	84.8	0.046	0.103	0.010	5.0	000526
9	(10, 6)	···	···	···	0.009	···	−117.3	0.036	0.160	0.010	5.5	000526
10	(−10, 6)	−12.5	0.051	0.157	0.010	6.9	−13.7	0.044	0.288	0.007	11.8	000526
11	(30, 30)	71.7	0.302	1.027	0.022	18.8	71.3	0.249	1.151	0.028	14.4	000530
12	(30, 30)	37.7	0.092	0.161	0.014	6.4	37.7	0.078	0.260	0.014	7.4	000530
13	(30, −30)	51.1	0.202	0.951	0.022	15.1	54.4	0.160	0.852	0.025	11.0	000531
14	(90, 0)	23.3	0.311	1.037	0.021	20.5	23.2	0.416	1.690	0.026	24.3	000531
15	(90, 0)	86.9	0.161	0.686	0.021	12.1	86.5	0.152	0.915	0.026	10.8	000531

* Observed telescope position.

and in the inner bulge (e.g., Deguchi et al. 2000a,b) revealed that approximately 2/3 of the SiO sources had not been detected previously in spite of a very sensitive OH 1612 MHz survey (Lindqvist et al. 1992a,b; Sevenster et al. 1997) with the VLA and the ATCA.

Large-amplitude variables (including long-period and semiregular variables, as well as supergiants) are potential candidates for SiO maser emitters. We compared the positions of SiO sources without OH identification with the known positions of the large-amplitude variables within 12′ of the Galactic center (Glass et al. 2001). The positions of these variables were measured with the K-band array camera, and are of a few arcsec accuracy. We found that 4 SiO sources (No. 1, 4, 12, and 14) are located near to these long-period variables within the estimated positional uncertainty. These identifications are given in columns 9 and 10 in table 2. Because the radial velocities of these large-amplitude variables are not known, the identifications of these sources may be slightly less certain than the OH identifications. So far, SiO sources No. 3, 5, 7, and 8 have no OH 1612 MHz counterpart and no corresponding large-amplitude variable; nevertheless, these were detected before in SiO by Izumiura et al. (1998).

We also checked the corresponding near-infrared objects in the 2MASS image server for unidentified sources. However, because the star density within 30″ of the Galactic center is too high [e.g., Blum et al. (1996)], it is quite difficult to identify the SiO sources in this region. On the 2MASS images, we could only find one red candidate (~ 10 mag in the K-band) for source No. 3 within a 5″ error circle. This red star, however, accompanies a faint extended ($\sim 5''$) feature which is considerably elongated in galactic longitude, probably because of the coalescence of several stars due to the low spatial resolution of the 2MASS images.

3.2. *Velocity Distribution of the SiO Masers Sources*

The bottom panel of figure 1 shows a longitude–velocity diagram for the 15 detected sources. The positions given in table 2 were used for making this diagram. A linear fit to the SiO radial velocities was made, and the result is given in the first row of table 3. There are two extreme sources with very large negative velocities, −336 and −308 km s^{-1}. It is possible that the sources with very large radial velocities are bulge stars with a very small angular momentum, rather than stars in the Galactic-center stellar cluster (van Langevelde et al. 1992; Izumiura et al. 1995). They may be located far from the Galactic center in distance, but happen to be seen near to it in projection, though this possibility is small. We also made a linear fit excluding these two sources. The results are also given in the second row of table 3.

The slope of about 1.1(±0.5) km s^{-1} per arcsec (or 3890 km s^{-1} deg^{-1}, or a rotation period of 2.3×10^5 yr around the Galactic center) is a factor of a few larger than the previously obtained values from SiO and OH maser observations on much larger scales [e.g., Miyazaki et al. (2001)]. Even for the sample excluding the 2 extreme-velocity sources, the slope is ~ 2290 km s^{-1} deg^{-1}. The present value of the slope is not compatible with the previously obtained low value by Izumiura et al. (1998) (~ 0.09 km s^{-1} per arcsec), probably because the positions of the sample in Izumiura et al. (1998) were not known to an accuracy better than the telescope beam size of about 40″; the positional accuracy was considerably better in our present observation. The obtained high rotational speed of the SiO maser cluster is, however, simply the slope of the least-squares fit, and must be interpreted very carefully. Non-circular motions of stars and the gravitational potential made from the central compact mass and the nuclear star cluster are responsible for the observed velocity structure. The high rotational

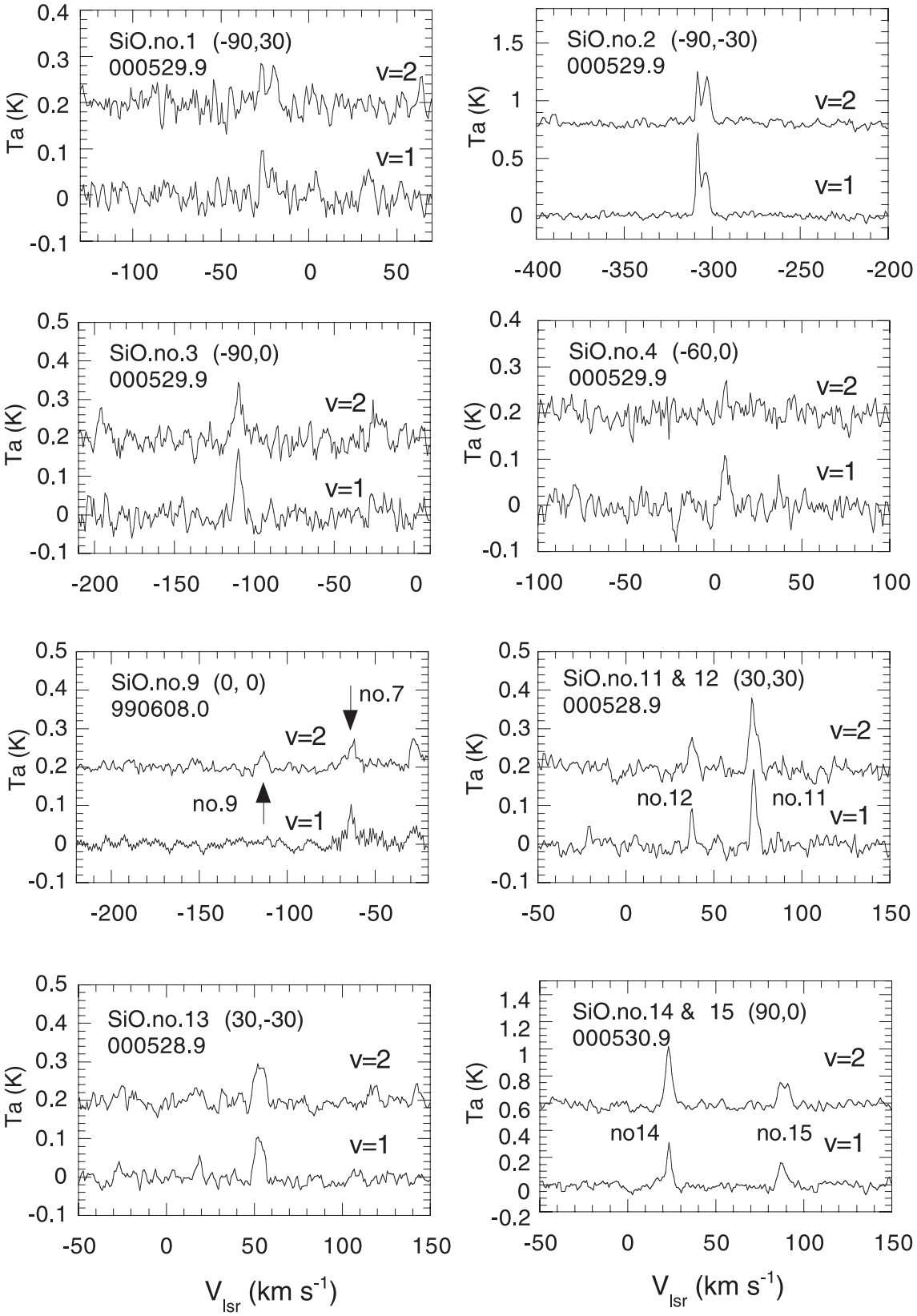

Fig. 3. SiO maser spectra of the detected sources. The source number shown at the upper left of each panel corresponds to the number in tables 1 and 2. The observed positions (in unit of arcsec from Sgr A*) are shown in parentheses.

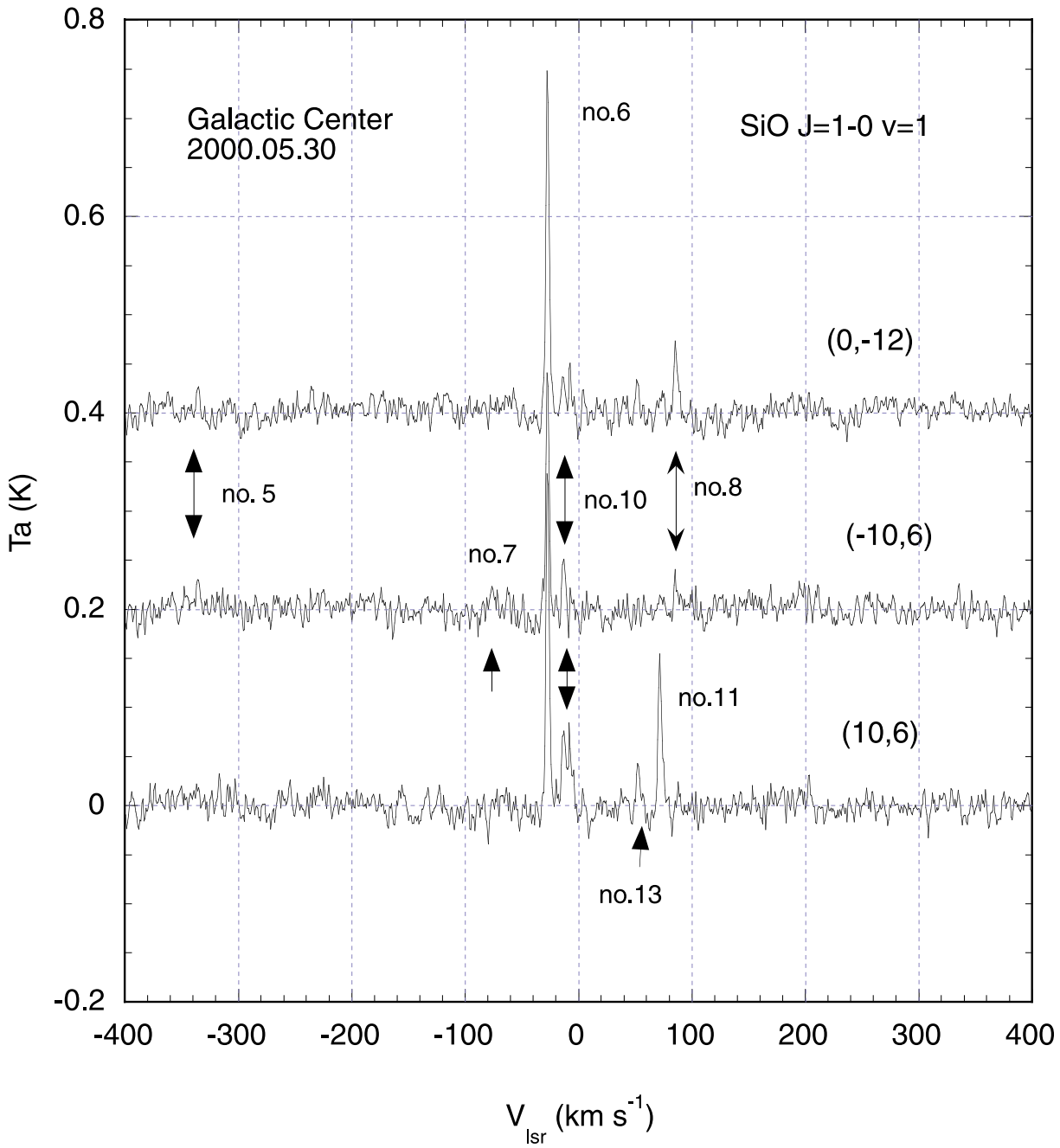

Fig. 4. SiO spectra in the $J = 1$–0 $v = 1$ transition at the three $12''$-offset positions around Sgr A*. The position offsets from Sgr A* in unit of arcsec are shown on the right side. The component number in this figure corresponds to the number given in tables 1 and 2.

speed of these stars is comparable to the rotational velocity of the circumnuclear gas ring which has been observed in various molecular lines [e.g., Wright et al. (2001)]. It is possible that these rapidly rotating AGB stars were born as a result of star formation in the circumnuclear ring (Levine et al. 1995).

The velocity dispersion from the average linear fit is approximately $108\,\mathrm{km\,s^{-1}}$ (or $54\,\mathrm{km\,s^{-1}}$ excluding the extreme sources). This value gives the mass of the Galactic center (integrated to $100''$; $\sim 4.1\,\mathrm{pc}$) as $\sim 1 \times 10^7\,M_\odot$, when we use the virial theorem, which is consistent with previous estimates of the mass of the Galactic center region (Krabbe et al. 1995; Morris, Serabyn 1996). The radial velocity dispersion obtained for SiO maser sources, $110\,\mathrm{km\,s^{-1}}$, is slightly smaller than the value of $154\,\mathrm{km\,s^{-1}}$ for the late-type stars within $12''$ from the Galactic center (Krabbe et al. 1995). In fact, if we take the SiO sources only within a $20''$ radius from the Galactic center in our sample (No. 5–10; including the extreme source No. 5), we get a velocity dispersion of $133\,\mathrm{km\,s^{-1}}$, giving a reasonable agreement with the result of Krabbe et al. (1995).

A simple judgement on whether or not a particular star is dynamically bound to the Galactic-center massive compact object can be obtained from the characteristic binding energy per

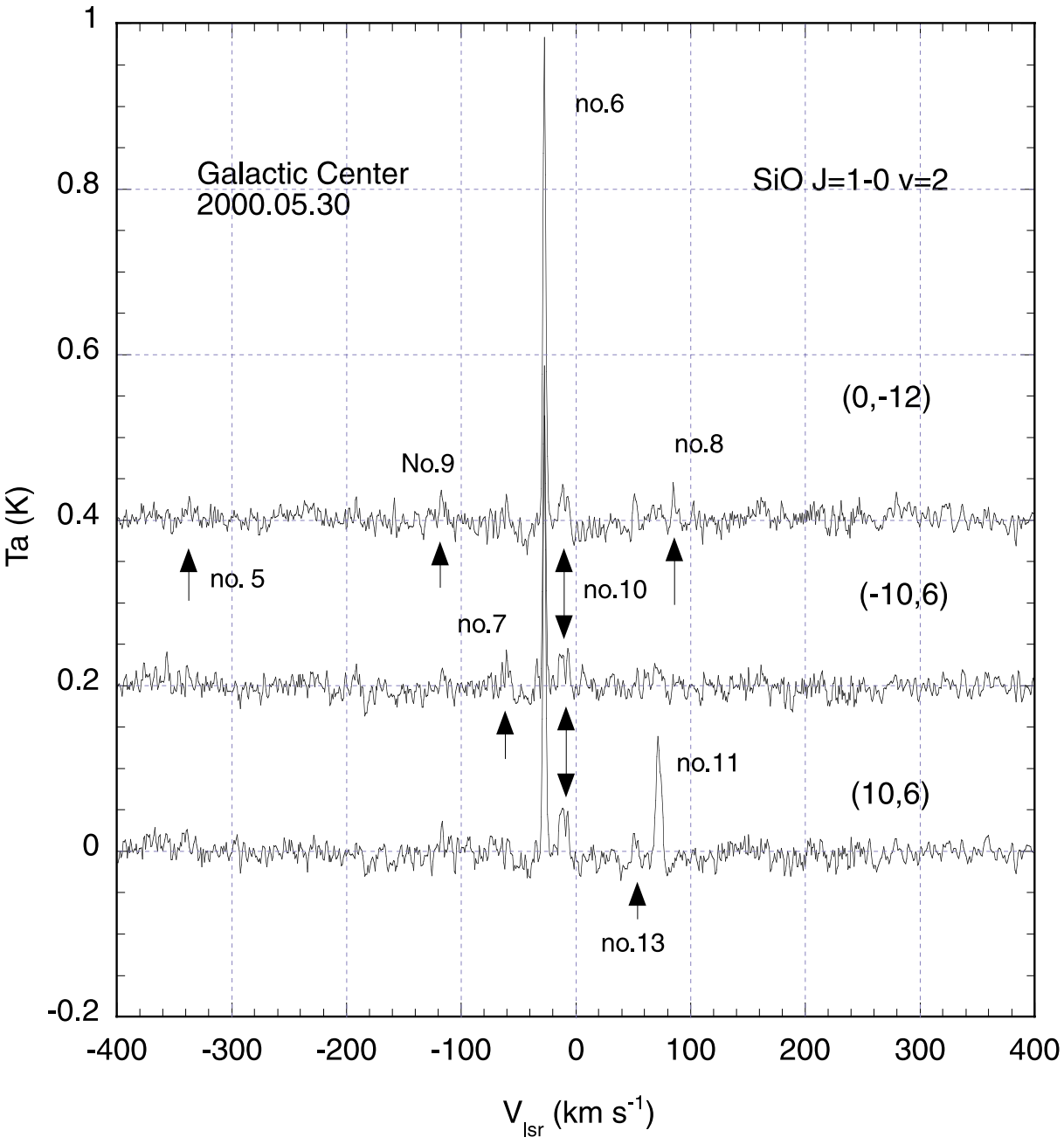

Fig. 5. Same as figure 4, but for the $J = 1$–0, $v = 2$ transition.

unit mass, $E_c = (1/2)V_{l.o.s.}^2 - GM/r_p$. Here, $V_{l.o.s.}$, r_p, G, and M are the observed radial velocity, the projected radius from the galactic center, the gravitational constant, and the mass of the central compact object (for which we adopt $2.8 \times 10^6\, M_\odot$; Ghez et al. 2000; Genzel et al. 2000), respectively. Considering a perpendicular velocity component and some depth along the line of sight, the characteristic binding energy, E_c, gives a lower limit to the real binding energy when the central mass dominates the gravitational field. For the SiO sources (No. 2, 3, and 15), the characteristic binding energies are positive. Therefore, these sources are not dynamically bound to the central compact object.

Because the SiO intensity of the extreme object No. 5 was quite weak in the year 2000, the position uncertainty given in the present paper is quite large. The characteristic binding energy of object No. 5 could be positive if the true position is a few arcsec further away from the Galactic center than that observed. The SiO intensity of this component was much stronger in 1997 (Izumiura et al. 1998). Therefore, a more accurate position should be obtained at a future date.

3.3. Time Variation

The intensities of SiO maser lines change significantly on a time scale of one year. Though the number of SiO sources detected in this study was similar to the number given previously (Izumiura et al. 1998), the two lists are not completely

Table 2. Obtained positions and identifications to the previously detected objects.

No.	l (°)	b (°)	Δl (″)	Δb (″)	$(\Delta l)_{\rm er}$ (″)	$(\Delta b)_{\rm er}$ (″)	$V_{\rm lsr}^{\rm SiO}$ (km s^{-1})	Ref.*	Identification† (km s^{-1})	$V_{\rm lsr}^{\rm Ref}$ (km s^{-1})	Δr (″)
1	359.915	−0.041	−105	18	7	5	−26.7	3	3–57		6
2	359.919	−0.055	−92	−32	5	5	−308.1	1, 3	359.918−0.055, 3–2855	−307.9	5
3	359.921	−0.047	−84	−3	5	5	−110.1	2, 3	M4	−105.1	
4	359.930	−0.045	−47	0	5	7	6.9	2,3	M3, 3–88	17.5	6
5	359.944	−0.045	0	4	10	9	−335.8	2	C7	−341.9	
6	359.945	−0.047	2	−2	11	11	−27.6	1,2,4	359.946−0.048, C4, IRS10EE	−26.4	6
7	359.945	−0.045	2	3	14	12	−61.4	2	C5	−69.6	
8	359.946	−0.046	5	−1	18	13	85.0				
9	359.946	−0.047	5	−4	12	8	−117.3	2,4	C6, IRS7	−121	7
10	359.946	−0.045	6	3	13	15	−13.1	2,4	C2, IRS15NE	−14.6	5
11	359.952	−0.040	28	22	8	5	71.5	1,2	359.954−0.041, P1	70.6	10
12	359.953	−0.032	30	52	6	30	37.7	3	3–885		8
13	359.957	−0.051	46	−19	5	5	52.8	1, 2, 3, 5	359.956−0.050, P2,3–5	48.5	8
14	359.970	−0.043	93	10	8	5	23.3	3	3–6		3
15	359.973	−0.048	105	−8	12	5	86.7	1, 3	359.970−0.049,3–3	88.8	8

* References: 1 — Sjouwerman et al. (1998b), 2 — Izumiura et al. (1998), 3 — Glass et al. (2001), 4 — Menten et al. (1997), 5 — Levine et al. (1995).
† The names, 3–57, etc. (indicating the survey field and the star number) refer to the large-amplitude variables in Glass et al. (2001). The names of the sources in Izumiura et al. (1998) are designated as Mn, Cn, and Pn, where M, C, and P stand the telescope positions at $(-40'', 0)$, $(0'', 0'')$, and $(+40'', 0)$, respectively, relative to Sgr A*, and n the number given to the detected SiO source in Izumiura et al. (1998).

Table 3. Fitting results.

Sample	Number of sources	Best fit (km s^{-1})	r.m.s. (km s^{-1})
All sources (including extreme sources)	15	$-42.0(\pm30.0) + 1.07(\pm0.51)[\Delta l('')]$	108.4
Low-velocity sources only (excluding extreme sources)	13	$-3.7(\pm16.3) + 0.67(\pm0.28)[\Delta l('')]$	53.9

the same; 9 objects in the SiO spectra in 2000 are inferred to be the same as those found in 1997 because of velocity coincidences. The identifications are given in columns 9 and 10 of table 2. If we compare figure 1 in the present paper with the middle panel of figure 1 of Izumiura et al. (1998), we can recognize significant variations in SiO maser intensities during the last 5 years.

We noticed in 2000 March that the SiO masers of source No. 6 (the $-27\,{\rm km\,s^{-1}}$ component, known as IRS 10 EE; Menten et al. 1997) had flared up to more than $T_{\rm a} \simeq 0.5\,{\rm K}$ ($\sim 1.5\,{\rm Jy}$). The SiO maser intensities of source No. 6 are plotted against time in figure 6. We took the 1996 and 1997 data from Menten et al. (1997) and Izumiura et al. (1998), respectively, and the 2000 March–April data from Miyazaki et al. (2001). The peak and integrated intensities of the $-27\,{\rm km\,s^{-1}}$ component of Miyazaki et al. (2001) agree quite well with the 2000 May results in this work. Therefore, the flare lasted for more than two months, from the end of 2000 March to the end of 2000 May. Because we did not observe the Galactic center in 1998, it is not known if there was any brightening in 1998. Near-infrared monitoring observations of this source over an interval of 4 years (Wood et al. 1998; assigned as LWHM65) gave a period of 736 days for the light variation. Extrapolating the fit of the light curve given in Wood et al. (1998), we estimate that the infrared maxima of this source came around mid November of 1998 and late November of 2000. However,

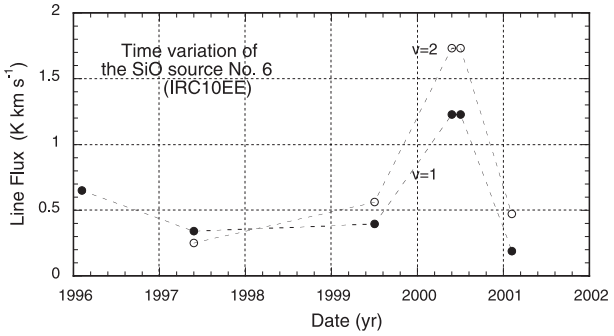

Fig. 6. Time variation of the SiO lines from No. 6 (IRS 10 EE). The data of 1996 and 1997 were taken from Menten et al. (1997) and Izumiura et al. (1998). The data of 2000 March were taken from Miyazaki et al. (2001). The filled and unfilled circles indicate the SiO J = 1–0, v = 1 and 2 lines, respectively. The line fluxes in 1997 and 1999 were scaled by a factor of 1.4 because IRS 10 EE is located at an offset of about 10″ from Sgr A*.

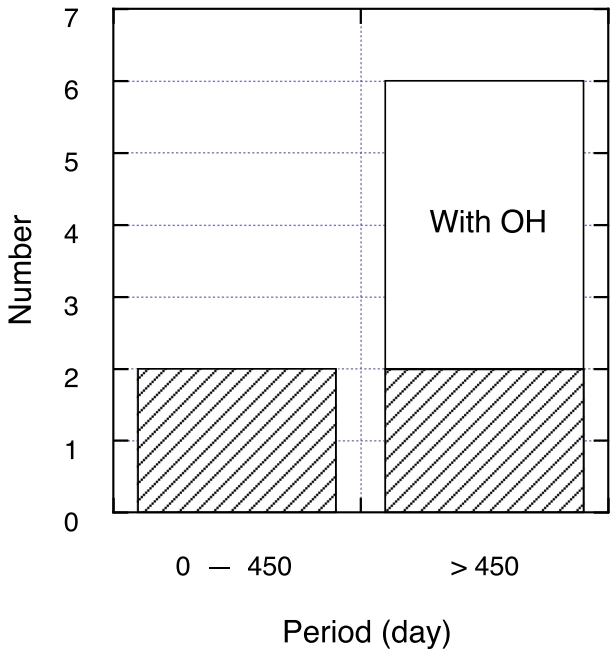

Fig. 7. Histogram of the periods for the SiO detected sources. The blank and shadow parts indicate the SiO sources with and without OH counterparts. All of the SiO sources with OH counterparts are stars with periods longer than 450 days.

because the observed light curve (Wood et al. 1998) has a large ambiguity, the estimated time of the light maximum is quite uncertain. It may have occured in advance by several months before 2000 November (in fact, 2000 March–June), if we assume that the light maximum occurs at the same time as the SiO maser intensity maximum.

The intensities of the SiO lines from IRS 10 EE, $T_{\rm a} \simeq 0.5\,{\rm K}$ (about 1.5 Jy), in 2000 May were comparable to the intensity of the SiO $J = 1$–0 $v = 1$ maser from Sgr B2 MD5 (Shiki et al. 1997; Morita et al. 1992). If they are scaled to a distance of 500 pc ($\sim 400\,{\rm Jy}$), they are comparable with the intensities of the Orion SiO masers. Therefore, the SiO maser flare of IRS 10 EE may indicate that the mass-loss rate of this star is temporarily enhanced to rates comparable to those from Orion IRc2 and Sgr B2 MD5. If the flare of IRS 10 EE is repeated periodically, it is probably associated with a pulsation activity of the central star. If it is irregular, it is possible to consider another mechanism, for example, a wind–wind collision between nearby massive stars (Yusef-Zadeh, Melia 1992). In addition, a tidal effect due to a close encounter between nearby stars might not be negligible, because the density of stars in the central star cluster is quite high.

For the 8 SiO sources (No. 1, 2, 4, 6, 12, 13, 14, and 15), the periods of light variation are known (Blommaert et al. 1998; Wood et al. 1998; Glass et al. 2001). A histogram of the periods is shown in figure 7. Because the sample involves only 8 stars, we divided it into two bins, i.e., above and below 450 days. It is worth mentioning that all sources with OH counterparts have periods of more than 450 days (see figure 7). Note that the average period of the sample with 412 large-amplitude variables near the Galactic center given by Glass et al. (2001) is 427 days. Therefore, the Galactic-center SiO source sample is probably weighted more toward those variables with longer periods than the average. SiO masers are, however, occasionally detected in stars with shorter periods than those in which OH masers were found. Considering the mass–luminosity–period relation [e.g., Vassiliadis, Wood (1993)], we conclude that lower-mass AGB stars are more often detected in SiO maser observations than in OH 1612 MHz observations. Because the size of the sample is slightly small, the conclusion may not be free from statistical fluctuations. However, the present conclusion is quite consistent with the finding by Glass et al. (2001) that the OH 1612 MHz sources have longer periods than the average period in their sample. According to an SiO maser study of the Galactic disk IRAS sources (Nakashima, Deguchi 2001), stars with bluer colors in terms of the IRAS $25/12\,\mu$m intensity ratio (relatively thin dust envelope) tend to be detected in SiO masers more often than in OH 1612 MHz masers. This fact also seems to agree qualitatively with the above result for the Galactic-center AGB stars, though the IRAS $25/12\,\mu$m colors do not necessarily correlate well with the periods of AGB stars (Whitelock et al. 1991; Nakashima et al. 2000).

The total number of SiO sources detected in the present paper is 15. If we include all of the SiO sources which were detected by Izumiura et al. (1998) and in the present work, the total number of SiO maser stars in the region of $200'' \times 100''$ from the Galactic center is 20. Further monitoring observations of the SiO maser intensities of these Galactic center SiO sources are definitely required.

4. Conclusion

We have made mapping and monitoring observations of SiO maser sources near the Galactic center and have detected 15 SiO sources. Approximate positions were obtained with accuracies of about 5–10″; five sources were identified with the previously observed OH 1612 MHz sources. Among the sources without OH counterparts, four are close to the positions of the large-amplitude variable stars observed at near-infrared wavelengths and two to previously detected SiO sources with accurate positions from the VLA. Three-year monitoring observations of these objects found that SiO masers from IRS 10 EE flared up by a factor of more than 5 during 2000 March–May. A least-squares linear fit of the velocities to the Galactic longitude in the longitude–velocity diagram gives a high rotational speed for the star cluster around the Galactic center.

The authors thank I. Glass for stimulating discussions and reading the manuscript. They also thank M. Morris, H. Izumiura, H. Imai, and A. Miyazaki for comments. This research was partly supported by Scientific Research Grant (C2) 12640243 of Japan Society for Promotion of Sciences.

References

Beckert, T., Duschl, W. J., Mezger, P. G., & Zylka, R. 1996, A&A, 307, 450

Blommaert, J. A. D. L., van der Veen, W. E. C. J., van Langevelde, H. J., Habing, H. J., & Sjouwerman, L. O. 1998, A&A, 329, 991

Blum, R. D., Sellgren, K., & DePoy, D. L. 1996, ApJ, 470, 864

Deguchi, S., Fujii, T., Izumiura, H., Kameya, O., Nakada, Y., Nakashima, J., Ootsubo, T., & Ukita, N. 2000a, ApJS, 128, 571

Deguchi, S., Fujii, T., Izumiura, H., Kameya, O., Nakada, Y., & Nakashima, J. 2000b, ApJS, 130, 351

Eckart, A., & Genzel, R. 1997, MNRAS, 284, 576

Genzel, R., Pichon, C., Eckart, A., Gerhard, O. E., & Ott, T. 2000, MNRAS, 317, 348

Genzel, R., Thatte, N., Krabbe, A., Kroker, H., & Tacconi-Garman, L. E. 1996, ApJ, 472, 153

Ghez, A. M., Morris, M., Becklin, E. E., Tanner, A., & Kremenek, T. 2000, Nature, 407, 349

Glass, I. S., Matsumoto, S., Carter, B. S., & Sekiguchi, K. 2001, MNRAS, 321, 77

Izumiura, H., Deguchi, S., & Fujii, T. 1998, ApJ, 494, L89

Izumiura, H., Deguchi, S., Hashimoto, O., Nakada, Y., Onaka, T., Ono, T., Ukita, N., & Yamamura, I. 1995, ApJ, 453, 837

Krabbe, A., Genzel, R., Eckart, A., Najarro, F., Lutz, D., Cameron, M., Kroker, H., Tacconi-Garman, L. E., et al. 1995, ApJ, 447, L95

Levine, D. A., Figer, D. F., Morris, M., & McLean, I. S. 1995, ApJ, 447, L101

Lindqvist, M., Habing, H. J., & Winnberg, A. 1992a, A&A, 259, 118

Lindqvist, M., Winnberg, A., Habing, H. J., & Matthews, H. E. 1992b, A&AS, 92, 43

Lindqvist, M., Winnberg, A., Johansson, L. E. B., & Ukita, N. 1991, A&A, 250, 431

Menten, K. M., Reid, M. J., Eckart, A., & Genzel, R. 1997, ApJ, 475, L111

Miyazaki, A., Deguchi, S., Tsuboi, M., Kasuga, T., & Takano, S. 2001, PASJ, 53, 501

Morita, K.-I., Hasegawa, T., Ukita, N., Okumura, S. K., & Ishiguro, M. 1992, PASJ, 44, 373

Morris, M., & Serabyn, E. 1996, ARA&A, 34, 645

Nakashima, J., & Deguchi, S. 2001, PASJ, submitted

Nakashima, J., Jiang, B. W., Deguchi, S., Sadakane, K., & Nakada, Y. 2000, PASJ, 52, 275

Rogers, A. E. E., Doeleman, S., Wright, M. C. H., Bower, G. C., Backer, D. C., Padin, S., Philips, J. A., Emerson, D. T., et al. 1994, ApJ, 434, L59

Sevenster, M. N., Chapman, J. M., Habing, H. J., Killeen, N. E. B., & Lindqvist, M. 1997, A&AS, 122, 79

Shiki, S., Ohishi, M., & Deguchi, S. 1997, ApJ, 478, 206

Sjouwerman, L. O., van Langevelde, H. J., & Diamond, P. J. 1998a, A&A, 339, 897

Sjouwerman, L. O., van Langevelde, H. J., Winnberg, A., & Habing, H. J. 1998b, A&AS, 128, 35

Sofue, Y., Inoue, M., Handa, T., Tsuboi, M., Hirabayashi, H., Morimoto, M., & Akabane, K. 1986, PASJ, 38, 475

van Langevelde, H. J., Brown, A. G. A., Lindqvist, M., Habing, H. J., & de Zeeuw, P. T. 1992, A&A, 261, L17

Vassiliadis, E., & Wood, P. R. 1993, ApJ, 413, 641

Whitelock, P., Feast, M., & Catchpole, R. 1991, MNRAS, 248, 276

Wood, P. R., Habing, H. J., & McGregor, P. J. 1998, A&A, 336, 925

Wright, M. C. H., Coil, A. L., McGary, R. S., Ho, P. T. P., & Harris, A. I. 2001, ApJ, 551, 254

Yusef-Zadeh, F., & Melia, F. 1992, ApJ, 385, L41